Journal of Chemical Health Risks

www.jchr.org

JCHR (2025) 15(5), 3324-3334 | ISSN:2251-6727

Impact of High Charcoalization Temperature on Textural and Physiochemical Properties of Orange Peel Derived Biochars

Anamika Kumari[1], Navneet Kumar*[2]

[1] Research Scholar, Department of Chemistry, Faculty of Engineering, Teerthankar Mahaveer University, Moradabad, Uttar Pradesh 244001, India.

[*2]Associate Professor, Department of Chemistry, Faculty of Engineering, Teerthankar Mahaveer University, Moradabad, Uttar Pradesh 244001, India.

***Corresponding Author: Navneet Kumar[2*]**

2*Associate Professor, Department of Chemistry, Faculty of Engineering, Teerthankar Mahaveer University, Moradabad, Uttar Pradesh 244001, India.

(Received: 27 September 2025 Revised: 05 October 2025 Accepted: 14 October 2025)

KEYWORDS

Biochar

Charcoalization

Ph

Surface Area

Orange Peel

ABSTRACT:

This study delved into the impact of high charcoalization temperature on textural and physiochemical properties of biochars extracted from Orange Peel (OP) and Orange Peel impregnated with $ZnCl_2$ (OP-$ZnCl_2$). The formation of biochars was occurred at three charcoalization temperatures of 600, 800, and 1000 ° C. As charcoalization temperature increased, pH of biochars elevated from mildly basic to exceedingly basic. The surface area of the biochar extracted from Orange peel expanded from 0.28 to 419.94 m^2g^{-1} and 0.95 to 673.47 m^2g^{-1} for biochar extracted from Orange peel modified with $ZnCl_2$ as charcoalization temperature increased. Biochar extracted from modified orange peel by $ZnCl_2$ at higher charcoalization temperatures had observable pores of varying dimension and configuration. There were superimposed D_{band} and G_{band} in Raman spectra for all the biochars. XPS investigation showed as charcoalization temperature increased, a noticeable deduction in the percentage of oxygen occurred. High charcoalization temperatures can amplify the adequate efficiency of a biochar extracted from Orange Peel modified with $ZnCl_2$ as an adsorbent.

1. Introduction

Biochar is highly porous carbon matter that is generated through the heating of organic matter in a low-oxygen environment at high temperatures [1], [2]. Biochar exhibits properties, including surface area, porous structure, thermal obstinacy, electrical conductivity, functional groups on surface, volatility, fixed carbon percentage, and pH. These characteristics make biochar suitable for liquid-phase adsorption. Biochars potential as an economically affordable adsorption material for capturing pollutants in water is mostly dependent on its porosity, surface area, and chemical properties [3]. The use of biochars extracted from rice straw to remove tetracycline from water was generated at various temperatures of 350, 550, and 750 ° C. The research demonstrated that the biochar made at 750 ° C had the highest removal efficiency, ranging from 92.8 % to 96.7 %. This was due to its larger surface area compared to the alternative biochars [4]. A study suggested that how biochars made from woody biomass at 500 ° C, with and without MgO modification to adsorb phosphorous [5]. The results showed a significant increase in phosphorous adsorption capacity after impregnation with MgO, from 1.87-.71 mg/g to 27.91-28.98 mg/g. This improvement was linked to the larger surface area from 0.25-9.12 m^2g^{-1} to 21.91-27.98 m^2g^{-1} after infusion, playing a major role in increasing phosphorous adsorption. The empirical, chemical, and textural features of biochar can be enhanced by

Journal of Chemical Health Risks

www.jchr.org

JCHR (2025) 15(5), 3324-3334 | ISSN:2251-6727

adjusting the charcoalization temperatures during its production. The selection of charcoalization temperatures aims to maximize the breakdown of pyrolysis outputs. According to various studies, the maximum yield of pyrolysis outputs is attained within a temperature interval of 450 º C to 600 º C [6], [7], [8]. Although output of thermolysis products are maximized within this temperature limits, the properties of biochar are not completely realized, which can compromise its ability in different applications. Nevertheless, increasing the charcoalization temperature can improve its properties. Research has shown that higher charcoalization temperatures promote the formation of more complex aromatic ring structures in biochar, where isolated rings merge into imperfect sheets of condensed rings that can stack together to form crystalline structures [2], [9].The degree of merging aromatic rings into larger, more complex units has significant impact on biochar's obstinacy to thermal degradation [2]. As the number of carbon-carbon double bonded and aromatic structures increases, while the number of carbon-carbon single bonded structures decreases, biochar becomes more thermally stable. As charcoalization temperature increases, the pH values of the biochars increased. This increase in pH was notable in biochars extracted from Arundo donax, where the release of volatile compounds during charcoalization led to a concentration of basic substances, contributing to the higher pH values [10]. The surface area of biochars produced from Southeast Asian fruitwood chips rose from 2.56 to 220 m^2/g, as the charcoalization temperature rises from 349 to 551º C [11]. This increase in surface area at 550 º C was attributed to the partial charcoalization of biomass at lower temperatures, where pores were clogged with tarry residues. Hence, higher temperatures enabled the formation of more pores and the discharge of volatile compounds, resulting in a larger surface area. Therefore, this study delved into the impact of high charcoalization temperature on textural and physiochemical properties of biochars extracted from Orange Peel and Orange Peel impregnated with $ZnCl_2$. The choice of orange peel for this study is due to the fact that it is widely available as agricultural waste, low-cost material, and promotes sustainability [6]. OP has been used to remove heavy metals, dyes, pesticides, phenol and its derivatives from wastewater [12], [13], [14], [15]. The highest adsorption levels for Cu^{+2} and Cd^{+2} ions using OP were 2.81 mgg^{-1} and 2.61 mgg^{-1} respectively [16]. The percentage of metal ions removed diminished with a rise in their initial concentration. Another study suggested that the highest adsorption levels for Cu^{+2} and Cd^{+2} ions using OP modified by KCl were 59.77 mg/g and 126.10 mg/g respectively [17]. Orange zest may have lower removal efficiency as compared to other adsorbents. However, modification of orange peel with chemical agents has shown enhanced bioadsorption capacity.

2. Materials and Methods

2.1 Preparation of Biochar

Biochars were produced from orange peel and modified orange peel by $ZnCl_2$ named as OP and OP-$ZnCl_2$. The air drying of fresh orange peel samples was occurred for 2 days and then oven drying of the samples was occurred for 36 h at 100 º C. The particle size of oven dried samples was reduced by grinding. The grinded samples were divided into two parts. One part of the sample was mixed with $ZnCl_2$ solution of 1:2 ratios (50 g of sample was assorted with 100 g of solid $ZnCl_2$) in 500 mL distilled water. The solution was heated for 1 h at 90 º C. Then the solution was filtered and dried in oven for 48 h at 120 º C. The percentage of elements in samples is shown in Table 1.

Table 1: The Percentage of Elements in Orange Peel and Modified Orange Peel by $Zncl_2$

Element	OP	OP-$ZnCl_2$
Carbon	45.30	47.03
Hydrogen	5.45	6.54
Nitrogen	0.35	0.54
Oxygen	43.64	49.46

Journal of Chemical Health Risks

www.jchr.org

JCHR (2025) 15(5), 3324-3334 | ISSN:2251-6727

The charcoalization process involved heating of samples until the desired thermal level of 600, 800, and 1000 ° C at the speed of 5 ° $Cmin^{-1}$. The biochar samples were allowed to cool before being stored in sealed containers for further analysis. Biochars prepared from orange peel at charcoalization temperatures of 600, 800, and 1000 ° C were labelled as OP600, OP800, and OP1000 respectively. Similarly, OP-$ZnCl_2$600, OP-$ZnCl_2$800, and OP-$ZnCl_2$1000 are biochars prepared from modified orange peel by $ZnCl_2$ at charcoalization temperatures of 600, 800, and 1000 ° C respectively.

2.2 Thermal Obstinacy

The combustion of biochars in a thermogram instrument was occurred to determine the thermal obstinacy of biochars. About 7-10 mg of biochar was put in a combustion chamber and heated from 45 ° C to 850 ° C. Resistance index (R_{i50}) which is an expression of thermal obstinacy of biochar is given in Equation (1).

$$R_{i50} = \frac{T\ 50\ biochar}{T\ 50\ graphite} \quad (1)$$

The temperatures $T_{50\ biochar}$ and $T_{50\ graphite}$ mark the point where half of the biochar and graphite samples are oxidized [9], [18].

3. Results and Discussion

3.1 Composition of Elements

The composition of elements present in biochars prepared from orange peel and modified orange peel by $ZnCl_2$ at charcoalization temperatures of 600, 800, and 1000 ° C is shown in Table 2. The composition of atomic carbon and nitrogen increased while the composition of atomic hydrogen and oxygen decreased as charcoalization temperature increased. It is noticeable that the composition of carbon was increased as charcoalization temperature increased from 600 to 800 ° C for both biochars but there was no difference in percentage of carbon as charcoalization temperature increased from 800 to 1000 ° C for both biochars. This suggested that the composition of carbon reached a steady state as charcoalization temperature increased and further increase in charcoalization temperature has no effect on composition of atomic carbon of the biochar.

As charcoalization temperature increased, the composition of atomic oxygen decreased. This indicates the increase in aromaticity of the biochars. The reduced atomic oxygen implied more hydrophobicity. Increase in aromaticity suggested that isolated aromatic rings merged into an imperfect sheet of condensed aromatic rings that can stack up together to form crystalline structure [2], [19]. This same trend was observed in the biochar prepared from soybean biomass and pod at charcoalization temperatures of 350 and 650 ° C [20].

Table 2: Composition of Elements Present In Biochars Extracted From Orange Peel (OP) and Modified Orange Peel by $Zncl_2$ (OP-$Zncl_2$)

Element	OP600	OP800	OP1000	OP-$ZnCl_2$600	OP-$ZnCl_2$800	OP-$ZnCl_2$1000
Carbon	79.32	81.49	81.33	81.72	83.30	83.24
Hydrogen	2.66	2.45	1.89	2.92	2.74	2.10
Nitrogen	0.65	0.94	1.30	1.60	1.81	1.93
Oxygen	16.42	13.16	13.58	17.98	16.15	17.21

3.2 Thermal Obstinacy

The mass loss measurement showing thermal breakdown of the biochars are shown in Fig. 1. Resistance indexes (R_{i50}) of the biochars were calculated from the mass loss measurement graphs are shown in Table 3.

Journal of Chemical Health Risks
www.jchr.org
JCHR (2025) 15(5), 3324-3334 | ISSN:2251-6727

Table 3: Resistance index of biochars

Biochar	OP600	OP800	OP1000	OP-$ZnCl_2$600	OP-$ZnCl_2$800	OP-$ZnCl_2$1000
R_{i50}	0.48	0.48	0.64	0.48	0.48	0.72

Biochars had approximately same R_{i50} values at charcoalization temperatures of 600 and 800 ° C, whereas biochars had significantly higher R_{i50} values at charcoalization temperature of 1000 ° C. This suggested that resistance index increased as charcoalization temperature increased. A study suggested that the energy required to oxidize biochar depends on the bonding of carbon atom present in biochar [9]. Therefore, number of C-C single bonds in biochars are higher at charcoalization temperature of 600 and 800 ° C, while number of C=C double bonds in biochars are higher at charcoalization temperature of 1000 ° C which led to their higher thermal obstinacy. Resistance index categorize biochars into three thermal obstinacy groups; Category A (R_{i50}> 0.69) showing slightest resistant to organic decay, Category B (0.49< R_{i50}< 0.69) showing some resistant to organic decay, and Category C (R_{i50}< 0.49) showing highest resistant to organic decay [9].On the basis of this categorization, biochars at charcoalization temperature of 600 and 800 ° C fell in category C. On the other hand, biochar extracted from orange peel at charcoalization temperature of 1000 ° C fell in category B which shows some resistant to biodegradation, while biochar extracted from modified orange peel by $ZnCl_2$ at charcoalization temperature fell in category A which shows minimum resistant to biodegradation. Hence, OP-$ZnCl_2$1000 can be an appropriate choice for wastewater treatment as compared to OP1000. The biochars extracted from wheat straw and pig manure at charcoalization temperature of 250 ° C to 750 ° C had similar impact of charcoalization temperature on thermal obstinacy [21].

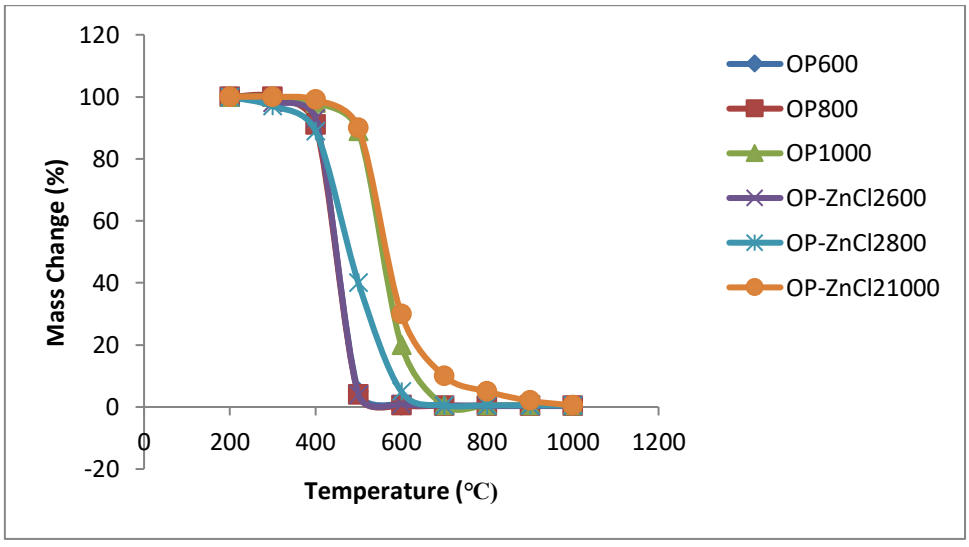

Fig. 1 Change in Mass Measurement Curves Of Samples Extracted From Orange Peel And Modified Orange Peel By $Zncl_2$

3.3 Surface area and pore size distribution

The BET surface area of biochars increased dramatically as charcoalization temperature increased. The significant rise in surface area of biochars is due to the chemical reaction triggered by charcoalization temperature whereby functional groups, including phenolic –OH, aromatic –CO, ester -C=O, aliphatic alkyl groups protecting the cores of aromatic structures are removed [22]. The BET surface area and pore volumes of biochars are shown in Table 4.

Journal of Chemical Health Risks
www.jchr.org
JCHR (2025) 15(5), 3324-3334 | ISSN:2251-6727

Table 4: Surface Area and Pore Volume of Biochars Extracted From Orange Peel and Modified Orange Peel by $Zncl_2$

Biochar	S_{BET} (m^2/g)	V_{total} (cm^3/g)	V_{micro} (cm^3/g)	V_{meso} (cm^3/g)	dp (nm)
OP600	0.28	-	-	-	-
OP800	26.70	0.06	0.03	0.04	0.72
OP1000	419.94	0.23	0.16	0.07	1.82
OP-$ZnCl_2$600	0.95	-	-	-	-
OP-$ZnCl_2$800	293.42	0.17	0.11	0.05	1.45
OP-$ZnCl_2$1000	673.47	0.39	0.23	0.16	2.05

*dp is average diameter of pore; V is pore volume; S is surface area

As charcoalization temperature rose, the total volume of pore of biochars expanded. During charcoalization process, volatile components of biochars have been released to create pores. It is noteworthy that the tarry residues which were clogging pores are reduced at higher charcoalization temperatures [23]. There were no pores detected in biochars at charcoalization temperature of 600 ° C, this may be due to lower surface area of the biochars at 600 ° C. Pore diameter distribution graph is shown in Fig. 2. This graph interpreted the non-uniformity of porous structure of biochars [24]. This graph also gives insights about distribution of total volume of pore are being smaller pore size or medium pore size [25]. The biochars prepared at charcoalization temperature of 600 ° C (OP600 & OP-$ZnCl_2$600) shows a pore diameter between 0.3 to 1.1 nm, which suggested that both biochars are composed of micropores (Fig. 3A). Biochar, OP-$ZnCl_2$600 has shown a higher peak as compared to OP600 biochar which implies that biochar extracted from modified orange peel by $ZnCl_2$ carries more pores. The biochars prepared at charcoalization temperature of 800 and 1000 ° C shows pore diameter between 0 to 2 nm, which suggested that the biochars are composed of micropores (Fig. 3B). However, OP-$ZnCl_2$1000 biochar shows medium size pores as well since pore diameter had extended to 4 nm. There are two types of micropores; ultramicropores (pore diameter < 0.69 nm) and supermicropores (pore diameters between 0.69-1.99 nm) [26]. The biochars exhibited predominant pore sizes ranging from 0.49-0.61 nm, indicating a high fraction of ultramicropores.

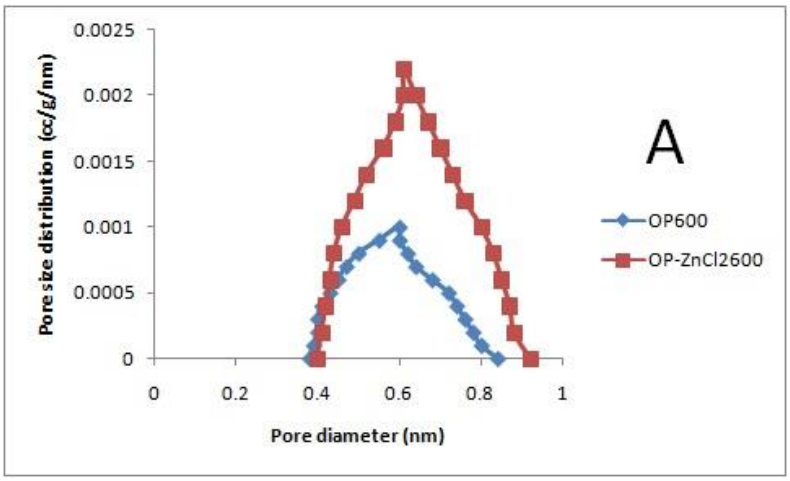

Journal of Chemical Health Risks
www.jchr.org
JCHR (2025) 15(5), 3324-3334 | ISSN:2251-6727

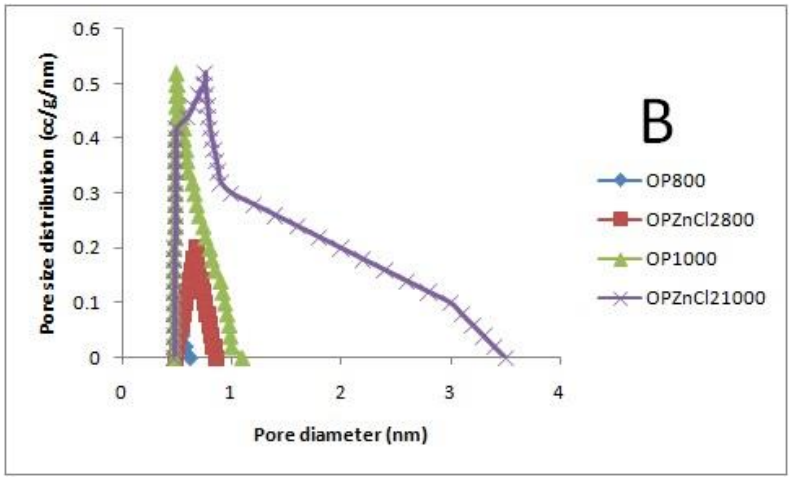

Fig. 2 Pore Diameter Distribution Graph of Biochars Extracted From Orange Peel And Modified Orange Peel By $Zncl_2$ (A) OP600 & OP-$Zncl_2$600; (B) OP800, OP-$Zncl_2$800, OP1000 & OP-$Zncl_2$1000

3.4 Analysis of surface terrain of the biochars

The structures of surface of biochars were analyzed by scanning electron microscope (SEM). SEM image of all the biochars were shown in Fig. 3. The release of volatile compounds present in biochars during charcoalization gave rise to the formation of pores in the biochars [6].The number of pores significantly increases in the biochar extracted from modified orange peel by $ZnCl_2$ as charcoalization temperature increases. Biochar, OP-$ZnCl_2$1000 has observable pores with different size. However, there were observable pores in biochars extracted from orange peel but in lesser extent as compared to the biochars extracted from modified orange peel by $ZnCl_2$. These pores acts as a medium which linked to the narrow apertures present on the internal face of the biochars [27]. The charcoalization temperature did not destroy the cellular structures of the biochars as the biochars have preserved the cell wall structures despite the increase in temperature.

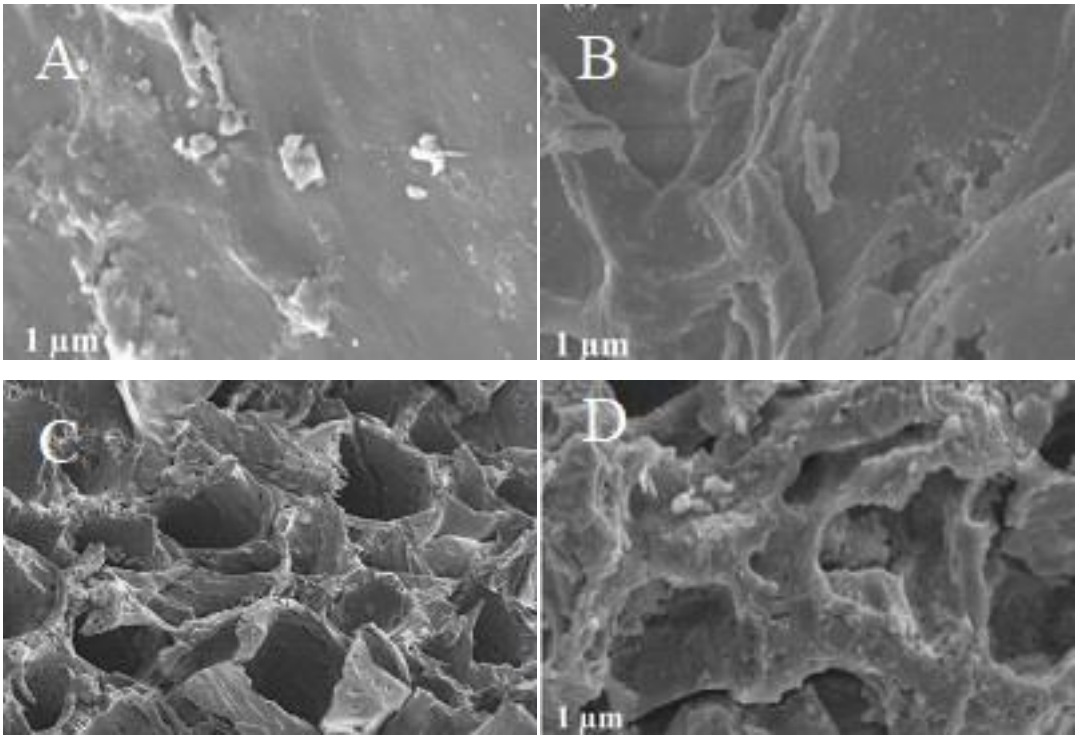

Journal of Chemical Health Risks

www.jchr.org

JCHR (2025) 15(5), 3324-3334 | ISSN:2251-6727

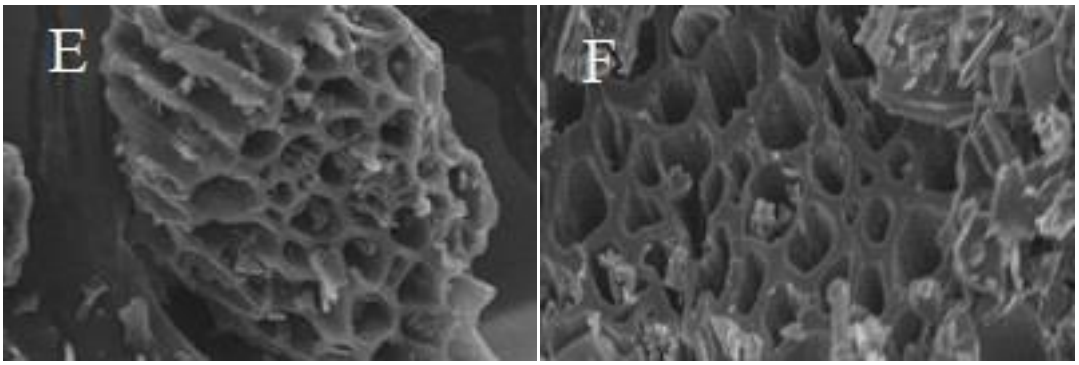

Fig. 3 SEM pictures of the biochars extracted from orange peel and modified orange peel by $ZnCl_2$ (A) OP600 (B) OP800 (C) OP1000 (D) OP-$ZnCl_2$600 (E) OP-$ZnCl_2$800 (F) OP-$ZnCl_2$1000

3.5 Analysis of molecular arrangement of the biochars

The molecular arrangement of the biochars was interpreted by Raman spectra shown in Fig. 4. All the spectra have two superimposed bands; G_{band} and D_{band}. G_{band} attributes to the crystallite structure while D_{band} attributes to the amorphous structure [21]. The location of G_{band}, D_{band}, and intensity ratio are shown in Table 5. Increasing the charcoalization temperature led to the decline in the location of D_{band} of the biochars, more so for OP-$ZnCl_2$. Nonetheless, there was no discrepancy in the location of G_{band} of the biochars. Intensity ratio is used to determine the degree of disordered carbon present in biochars with respect to graphite structure [28]. As charcoalization temperature increased, intensity ratio increased. It may be due to depolymerization reaction occurred during charcoalization. This increase in intensity ratio suggested the increase in lattice imperfection which accompanied the creation of oxygen containing reactive groups on the surface of biochars [29]. Biochars extracted from Japanese cedar also showed increase in intensity ratio as charcoalization temperature rose from 500 to 800 ° C, resulted in decreased size of crystalline domain [30].

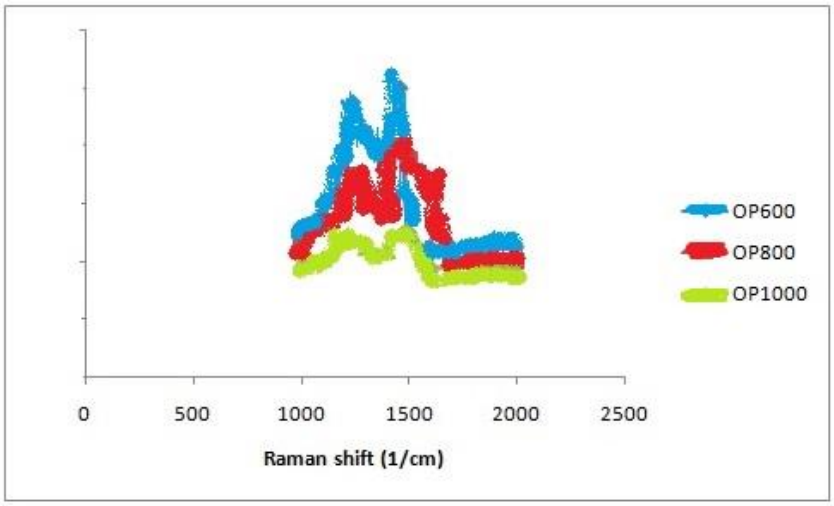

Journal of Chemical Health Risks

www.jchr.org

JCHR (2025) 15(5), 3324-3334 | ISSN:2251-6727

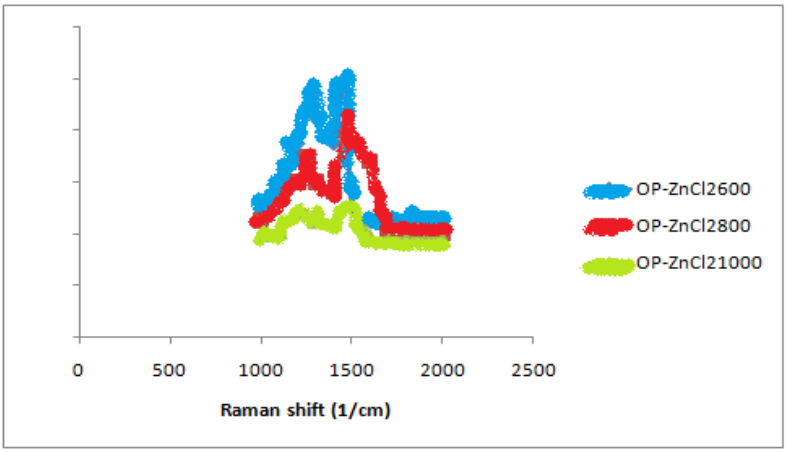

Fig. 4 Raman Spectra of Biochar Extracted From Orange Peel and Modified Orange Peel by $Zncl_2$

Table 5: Location of $G_{position}$ and $D_{position}$ and Intensity Ratio of Biochars Derived From Orange Peel and Modified Orange Peel by $Zncl_2$

Biochar	$G_{position}$ (cm^{-1})	$D_{position}$ (cm^{-1})	Intensity ratio (I_D/I_G)
OP600	1459.99	1239.85	0.62
OP-$ZnCl_2$600	1462.97	1290.85	0.62
OP800	1443.41	1226.37	0.86
OP-$ZnCl_2$800	1452.73	1254.38	0.77
OP1000	1496.00	1215.52	0.86
OP-$ZnCl_2$1000	1498.67	1216.37	0.89

3.6 Surface functionality

XPS scanning was used to inquire the results of high charcoalization temperature on surface capability of the biochars. Relative composition of decomposed functional groups C_{1s} and O_{1s} are shown in Table 6. There were three C_{1s} peaks for both biochars; peak 1 attributes to graphite carbon, peak 2 attributes to carbon present in alcohols, phenols or ethers functional groups and peak 3 attributes to carbon present in carbonyl, carboxyl, ester, quinine functional groups [27], [31]. As charcoalization temperature increased, peak 1 (graphite carbon) decreased whereas peak 3 corresponds to carbon in carboxylic, carbonyl, ester, quinine functional groups increased. The ratio of carbon present in functional group to graphite carbon was calculated to find out the fraction of surface containing carbon functional group per unit of graphite carbon. Raising the charcoalization temperature from 600 to 1000 ° C led to a rise in FC/GC ratio for both types of biochar (Table 6). Higher FC/GC ratio attributes to higher fraction of carbon functional groups relative to graphite carbon. Graphite carbon is hydrophobic while carbon functional groups are hydrophilic [32], [33], the fraction of carbon functional group and graphite carbon inferred to hydrophilicity or hydrophobicity of the biochar. Therefore, biochars at lower charcoalization temperature of 600 ° C were more water-repellent meanwhile biochars at higher charcoalization temperatures of 800 ° C and 1000 ° C were more water-attracting. There were three O_{1s} peaks for both biochars; peak 1 attributes to carbonyl oxygen present in quinine, peak 2 attributes to carbonyl oxygen present in ester, anhydride reactive groups and peak 3 attributes to non-carbonyl oxygen present in ester and anhydride reactive groups [34]. Higher charcoalization temperatures led to a decline in peak 1 and a rise in peak 3.

Journal of Chemical Health Risks

www.jchr.org

JCHR (2025) 15(5), 3324-3334 | ISSN:2251-6727

Table 6: XPS Analysis of Biochars Extracted From Orange Peel and Modified Orange Peel by $Zncl_2$

Biochar	C_{1s} (% wt.)				O_{1s} (% wt.)		
	$Peak_1$	$Peak_2$	$Peak_3$	FC/GC ratio	$Peak_1$	$Peak_2$	$Peak_3$
OP600	87.60	19.33	3.70	0.26	44.48	-	54.26
OP800	72.29	-	36.17	0.63	73.18	25.76	3.54
OP1000	61.46	-	45.54	0.77	77.06	21.43	1.60
OP-$ZnCl_2$600	94.83	8.71	5.97	0.37	57.98	-	86.15
OP-$ZnCl_2$800	59.00	-	44.00	0.79	73.19	21.09	8.87
OP-$ZnCl_2$1000	67.28	-	89.71	0.85	87.96	18.13	-

3.7 Effect of pH

The values of pH of the biochars were found to be between 9.69 and 12.16. It implied that biochars may be categorized as slightly basic to highly basic. Biochars, OP800 and OP-$ZnCl_2$1000 had the pH value of 10.16 and 12.16 sequentially. Biochars extracted from stems of corn, peanut, canola, and soybean at charcoalization temperature of 500 and 700 ° C had similar values of pH ranging from 9.39-11.32 [35]. Higher pH values of biochars suggested that basic residues of these biochars can be easily removed. The alkaline surface of biochars can be formed by decomposition of organic components at higher charcoalization temperatures [36], [37].

4. Conclusion

This study delved into the impact of high charcoalization temperature on textural and physiochemical properties of biochars extracted from Orange Peel (OP) and Orange Peel impregnated with $ZnCl_2$ (OP-$ZnCl_2$). The result of this study showed that biochar extracted from modified orange peel by $ZnCl_2$at high charcoalization temperatures had higher thermal obstinacy as compared to biochar extracted from orange peel. This study examined that there was an increase in composition of elements, BET surface area, total pore volume, pH, and functional groups present on surface of the biochars as charcoalization temperature increases. It implies that biochar extracted from modified orange peel by $ZnCl_2$ at high charcoalization temperatures will be a suitable adsorbent for wastewater treatment.

References

[1] Z. Liu and G. Han, “Production of solid fuel biochar from waste biomass by low temperature pyrolysis,” Fuel, vol. 158, pp. 159–165, Oct. 2015, doi: 10.1016/J.FUEL.2015.05.032.

[2] L. Leng and H. Huang, “An overview of the effect of pyrolysis process parameters on biochar stability,” Bioresour Technol, vol. 270, pp. 627–642, 2018, doi: https://doi.org/10.1016/j.biortech.2018.09.030.

[3] O. Oginni, K. Singh, and J. W. Zondlo, “Pyrolysis of dedicated bioenergy crops grown on reclaimed mine land in West Virginia,” J Anal Appl Pyrolysis, vol. 123, pp. 319–329, 2017, doi: https://doi.org/10.1016/j.jaap.2016.11.013.

[4] H. Wang et al., “Sorption of tetracycline on biochar derived from rice straw and swine manure,” RSC Adv, vol. 8, no. 29, pp. 16260–16268, 2018, doi: 10.1039/C8RA01454J.

[5] O. Oginni et al., “Phosphorus adsorption behaviors of MgO modified biochars derived from waste woody biomass resources,” J Environ Chem Eng, vol. 8, no. 2, p. 103723, 2020, doi: https://doi.org/10.1016/j.jece.2020.103723.

[6] O. Oginni and K. Singh, “Pyrolysis characteristics of Arundo donax harvested from a reclaimed mine land,” Ind Crops Prod, vol. 133, pp. 44–53, 2019, doi: https://doi.org/10.1016/j.indcrop.2019.03.014.

[7] I. Lewandowski, J. M. O. Scurlock, E. Lindvall, and M. Christou, “The development and current

status of perennial rhizomatous grasses as energy crops in the US and Europe," Biomass Bioenergy, vol. 25, no. 4, pp. 335–361, 2003, doi: https://doi.org/10.1016/S0961-9534(03)00030-8.

[8] X. Ge, F. Xu, J. Vasco-Correa, and Y. Li, "Giant reed: A competitive energy crop in comparison with miscanthus," Renewable and Sustainable Energy Reviews, vol. 54, pp. 350–362, 2016, doi: https://doi.org/10.1016/j.rser.2015.10.010.

[9] O. R. Harvey, L.-J. Kuo, A. R. Zimmerman, P. Louchouarn, J. E. Amonette, and B. E. Herbert, "An Index-Based Approach to Assessing Recalcitrance and Soil Carbon Sequestration Potential of Engineered Black Carbons (Biochars)," Environ Sci Technol, vol. 46, no. 3, pp. 1415–1421, Feb. 2012, doi: 10.1021/es2040398.

[10] R. Saikia, R. S. Chutia, R. Kataki, and K. K. Pant, "Perennial grass (Arundo donax L.) as a feedstock for thermo-chemical conversion to energy and materials," Bioresour Technol, vol. 188, pp. 265–272, 2015, doi: https://doi.org/10.1016/j.biortech.2015.01.089.

[11] Z. Chowdhury, M. Karim, M. Ashraf, and K. Khalisanni, "Influence of Carbonization Temperature on Physicochemical Properties of Biochar derived from Slow Pyrolysis of Durian Wood (Durio zibethinus) Sawdust," Bioresources, vol. 11, pp. 3356–3372, Feb. 2016, doi: 10.15376/biores.11.2.3356.

[12] N. Feng, X. Guo, S. Liang, Y. Zhu, and J. Liu, "Biosorption of heavy metals from aqueous solutions by chemically modified orange peel," J Hazard Mater, vol. 185, no. 1, pp. 49–54, 2011, doi: https://doi.org/10.1016/j.jhazmat.2010.08.114.

[13] F. Rahman, M. Akter, and M. Abedin, "Dyes removal from textile wastewater using orange peels," Int. J. Sci. Technol. Res., vol. 2, pp. 47–50, Jan. 2013.

[14] F. C. Ezeonu, G. I. Chidume, and S. C. Udedi, "Insecticidal properties of volatile extracts of orange peels," Bioresour Technol, vol. 76, no. 3, pp. 273–274, 2001, doi: https://doi.org/10.1016/S0960-8524(00)00120-6.

[15] L. Kumar et al., "Systematic studies on the effect of structural modification of orange peel for remediation of phenol contaminated water," Water Environ Res, vol. 95, p. e10872, Apr. 2023, doi: 10.1002/wer.10872.

[16] A. Yirga, O. P. Yadav, and T. Dey, "Waste Orange Peel Adsorbent for Heavy Metal Removal from Water," Pollution, vol. 8, no. 2, pp. 553–566, 2022, doi: 10.22059/poll.2021.331156.1193.

[17] X. Guo, S. Liang, and Q. Tian, "Removal of Heavy Metal Ions from Aqueous Solutions by Adsorption Using Modified Orange Peel as Adsorbent," Adv Mat Res, vol. 236–238, pp. 237–240, May 2011, doi: 10.4028/www.scientific.net/AMR.236-238.237.

[18] J. H. Windeatt, A. B. Ross, P. T. Williams, P. M. Forster, M. A. Nahil, and S. Singh, "Characteristics of biochars from crop residues: Potential for carbon sequestration and soil amendment," J Environ Manage, vol. 146, pp. 189–197, 2014, doi: https://doi.org/10.1016/j.jenvman.2014.08.003.

[19] M. Keiluweit, P. S. Nico, M. G. Johnson, and M. Kleber, "Dynamic Molecular Structure of Plant Biomass-Derived Black Carbon (Biochar)," Environ Sci Technol, vol. 44, no. 4, pp. 1247–1253, Feb. 2010, doi: 10.1021/es9031419.

[20] M. Ahmad et al., "Effects of pyrolysis temperature on soybean stover- and peanut shell-derived biochar properties and TCE adsorption in water," Bioresour Technol, vol. 118, pp. 536–544, 2012, doi: https://doi.org/10.1016/j.biortech.2012.05.042.

[21] L. Zhao, X. Cao, O. Mašek, and A. Zimmerman, "Heterogeneity of biochar properties as a function of feedstock sources and production temperatures," J Hazard Mater, vol. 256–257, pp. 1–9, 2013, doi: https://doi.org/10.1016/j.jhazmat.2013.04.015.

[22] B. Chen, D. Zhou, and L. Zhu, "Transitional Adsorption and Partition of Nonpolar and Polar Aromatic Contaminants by Biochars of Pine Needles with Different Pyrolytic Temperatures," Environ Sci Technol, vol. 42, no. 14, pp. 5137–5143, Jul. 2008, doi: 10.1021/es8002684.

[23] Y. Wang, Y. Hu, X. Zhao, S. Wang, and G. Xing, "Comparisons of Biochar Properties from Wood Material and Crop Residues at Different Temperatures and Residence Times," Energy & Fuels, vol. 27, pp. 5890–5899, Sep. 2013, doi: 10.1021/ef400972z.

[24] D. Prahas, Y. Kartika, N. Indraswati, and S. Ismadji, "Activated carbon from jackfruit peel waste by H3PO4 chemical activation: Pore structure and surface chemistry characterization," Chemical Engineering Journal, vol. 140, pp. 32–42, Jul. 2008, doi: 10.1016/j.cej.2007.08.032.

[25] O. Oginni, K. Singh, G. Oporto, B. Dawson-Andoh, L. McDonald, and E. Sabolsky, "Influence of one-step and two-step KOH activation on activated carbon characteristics," Bioresour Technol Rep, vol. 7, p. 100266, 2019, doi: https://doi.org/10.1016/j.biteb.2019.100266.

[26] E. N. Yargicoglu, B. Y. Sadasivam, K. R. Reddy, and K. Spokas, "Physical and chemical characterization of waste wood derived biochars," Waste Management, vol. 36, pp. 256–268, 2015, doi: https://doi.org/10.1016/j.wasman.2014.10.029.

[27] J. Xu, L. Chen, H. Qu, Y. Jiao, J. Xie, and G. Xing, "Preparation and characterization of activated carbon from reedy grass leaves by chemical activation with H3PO4," Appl Surf Sci, vol. 320, Dec. 2024, doi: 10.1016/j.apsusc.2014.08.178.

[28] Y.-R. Rhim et al., "Changes in electrical and microstructural properties of microcrystalline cellulose as function of carbonization temperature," Carbon N Y, vol. 48, no. 4, pp. 1012–1024, 2010, doi: https://doi.org/10.1016/j.carbon.2009.11.020.

[29] B. Peng et al., "Adsorption of Antibiotics on Graphene and Biochar in Aqueous Solutions Induced by π-π Interactions," Sci Rep, vol. 6, p. 31920, Aug. 2016, doi: 10.1038/srep31920.

[30] S. Yamauchi and Y. Kurimoto, "Raman spectroscopic study on pyrolyzed wood and bark of Japanese cedar: Temperature dependence of Raman parameters," Journal of Wood Science, vol. 49, pp. 235–240, Jun. 2003, doi: 10.1007/s10086-002-0462-1.

[31] E. Atta-Obeng, B. Dawson-Andoh, M. S. Seehra, U. Geddam, J. Poston, and J. Leisen, "Physico-chemical characterization of carbons produced from technical lignin by sub-critical hydrothermal carbonization," Biomass Bioenergy, vol. 107, pp. 172–181, 2017, doi: https://doi.org/10.1016/j.biombioe.2017.09.023.

[32] X. Xi, S. Jiang, W. Zhang, K. Wang, H. Shao, and Z. Wu, "An experimental study on the effect of ionic liquids on the structure and wetting characteristics of coal," Fuel, vol. 244, pp. 176–183, 2019, doi: https://doi.org/10.1016/j.fuel.2019.01.183.

[33] T. Oginni, K. Tingi, G. Oporto, B. Dawson-Andoh, L. McDonald, and E. Sabolsky, "Effect of one-step and two-step H3PO4 activation on activated carbon characteristics," Bioresour Technol Rep, vol. 8, p. 100307, Aug. 2019, doi: 10.1016/j.biteb.2019.100307.

[34] J.-H. Zhou et al., "Characterization of surface oxygen complexes on carbon nanofibers by TPD, XPS and FT-IR," Carbon N Y, vol. 45, no. 4, pp. 785–796, 2007, doi: https://doi.org/10.1016/j.carbon.2006.11.019.

[35] J. Yuan, R.-K. Xu, and H. Zhang, "The forms of alkalis in the biochar produced from crop residues at different temperatures," Bioresour Technol, vol. 102, pp. 3488–3497, Feb. 2011, doi: 10.1016/j.biortech.2010.11.018.

[36] A. T. Tag, G. Duman, S. Ucar, and J. Yanik, "Effects of feedstock type and pyrolysis temperature on potential applications of biochar," J Anal Appl Pyrolysis, vol. 120, pp. 200–206, 2016, doi: https://doi.org/10.1016/j.jaap.2016.05.006.

[37] D. Rehrah et al., "Production and characterization of biochars from agricultural by-products for use in soil quality enhancement," J Anal Appl Pyrolysis, vol. 108, pp. 301–309, 2014, doi: https://doi.org/10.1016/j.jaap.2014.03.008.